

# Synthesis of Carboxymethyl Chitosan and its Rheological Behaviour in Pharmaceutical and Cosmetic Emulsions

Desislava Tzaneva<sup>1</sup>, Apostol Simitchiev<sup>2</sup>, Nadezhda Petkova<sup>1\*</sup>, Ventzislav Nenov<sup>2</sup>, Albena Stoyanova<sup>3</sup>, Panteley Denev<sup>1</sup>

<sup>1</sup>Department of Organic Chemistry, University of Food Technologies, 26 Maritza Blvd., 4002, Plovdiv, Bulgaria.

<sup>2</sup>Department of Machinery for Food Industry, Technical Faculty, University of Food Technologies, 26 Maritza Blvd., 4002, Plovdiv, Bulgaria.

<sup>3</sup>Department of Essential Oils, University of Food Technologies, 26 Maritza Blvd., 4002, Plovdiv, Bulgaria.

## ARTICLE INFO

### Article history:

Received on: 28/06/2017

Accepted on: 15/09/2017

Available online: 30/10/2017

### Key words:

Carboxymethyl chitosan, FTIR spectroscopy, NMR spectra, TGA, emulsions, rheological and thermodynamic properties.

## ABSTRACT

The aim of the current study was synthesis and characterization of CMC and further evaluation of its emulsion stabilizing properties for preparation of pharmaceutical and cosmetic emulsions. Carboxymethyl chitosan (CMC) with high degree of substitution (50 %) has been synthesized and further characterization of resulting product by FTIR, NMR spectroscopy and thermal analysis (TGA/DTA) was carried out. CMC was also characterized as water soluble polymer with ability to give solutions with high viscosity. Rheological behavior of cosmetic emulsions prepared with 0.3 and 0.5 % CMC was investigated. Thermodynamic parameters of emulsions, Gibbs free energies, enthalpies and entropies have been calculated. The current study demonstrated use of CMC as stabilizer of emulsions with potential application in pharmaceutical and cosmetic oil/water emulsions.

## INTRODUCTION

Chitin is the secondmost abundant and renewable polysaccharide in nature only after cellulose (Kasaai *et al.*, 2013). Its chemical structure is similar to cellulose: both polysaccharides have  $\beta$ -(1 $\rightarrow$ 4) glycosidic linkages and they are able to form intermolecular hydrogen bonds. Chitin is highly crystalline and insoluble in common solvents. It is often converted into chitosan by deacetylation. The word "chitosan" is used for both partially and completely N-deacetylated chitins. Commercial chitin and chitosan are copolymers of 2-acetamido-2-deoxy-D-glucose (GlcNAc) and 2-amino-2-deoxy-D-glucose

(GlcN) with  $\beta$ -D-(1 $\rightarrow$ 4) glycoside linkages. The chemical structures of cellulose, chitin and chitosan are illustrated (Fig. 1).

"Green chemistry" with its part of biomaterials using natural polymers is developed with significant steps in and forms a promising field of research (Sharma *et al.*, 2017). Chitosan is an inexpensive and renewable material with many applications in cosmetics, pharmaceuticals, food science and biotechnology (Kim *et al.*, 2003; Lei *et al.*, 2003).

Due to the poor solubility of chitosan (only in acidic aqueous solutions below pH 6.5) its application is limited in many fields where solubility is a prime factor. The solubility of chitosan can be improved by depolymerization and its chemical modifications (Cravotto *et al.*, 2005). Chitosan contains reactive amino, primary and secondary alcohol groups that can be object of chemical modifications under mild reaction conditions to alter its properties (Mourya and Inamdar, 2008; Shanmuganathan *et al.*, 2016).

### \* Corresponding Author

Nadezhda Petkova, Department of Organic Chemistry, University of Food Technologies, 26 Maritza Blvd., 4002, Plovdiv, Bulgaria. E-mail: [petkovanadejda@abv.bg](mailto:petkovanadejda@abv.bg)

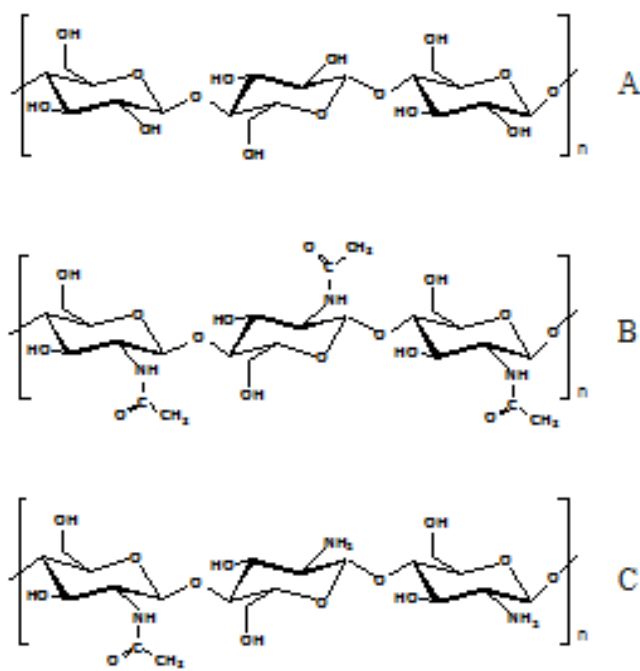


**Fig. 1:** Chemical structures of some polysaccharides: cellulose (A), chitin (B) and chitosan (C).

Many water-soluble derivatives have been prepared by quaternization (Jia *et al.*, 2001; Mourya and Inamdar, 2009) or by introducing hydrophilic groups like hydroxypropyl, dihydroxyethyl, hydroxyalkylamino (Jung *et al.* 1999; Kurita, 2001; Sashiwa *et al.*, 2003), sulfate (Holme and Perlin, 1997); phosphate, carboxyalkyl groups as carboxymethyl, carboxyethyl, carboxybutyl or by grafting water-soluble polymer (Yalpani *et al.*, 1991; Ouchi *et al.*, 1998; Park *et al.*, 2003; Mourya *et al.*, 2010) in the macromolecular chain of chitosan. Compared with other water-soluble chitosan derivatives, CMC has attracted much attention and has been widely studied because of its ease of synthesis, water solubility, ampholytic character and possibilities of wide range of application fields.

Carboxymethyl chitosan possesses not only a good solubility in water, but also has unique chemical, physical and biological properties such as high viscosity, large hydrodynamic volume, low toxicity, biocompatibility and good ability to form films, fibers and hydrogels (Muzzarelli, 1988; Chen *et al.*, 2005). The CMC can be in form of O-CMC, N-CMC and N,O-CMC (Mourya *et al.*, 2010). The properties and applications of CMC strongly depends on its structural characteristics, mainly the average degree of substitution and the position of the carboxymethylation (grafting to amino or hydroxyl groups) (de Abreu and Campana-Filho, 2005).

In recent years, the cosmetic industry has been a rapidly growing industry worldwide (Lee *et al.*, 2013). Continuous development of new active ingredients for cosmetics and personal care products is one of the most important areas of research in this industry (Cochran and Brockman 2007; Yang *et al.*, 2011). As a result, there are a significant number of novel cosmetic products that are based on a new generation of active ingredients (Patravale

and Mandawgade, 2008). Therefore, the potential applications of CMC in cosmetics will be viewed into five major uses as: moisture absorption-retention agent, anti-microbial agent, antioxidant agent, delivery system and oil/water emulsions stabilization (Ali *et al.*, 2013; Jimtaisong and Seawan, 2014).

The current study is focused on synthesis and characterization of CMC and further evaluation of its emulsion stabilizing properties for preparation of cosmetic and pharmaceutical emulsions.

## MATERIALS AND METHODS

Chitosan (molecular weight of 100 – 300 kDa) was purchased from Acros Organics (Belgium). Other chemicals and solvents (chloroacetic acid, sodium hydroxide, 2-propanol and methanol) were of analytical grade and were used without further purification.

### Characterization of chitosan

#### Degree of deacetylation

The degree of deacetylation was determined by conductometric titration (Ewing, 1969). In brief, the chitosan sample (500 mg) was stirred in 150 mL 0.5 M hydrochloric acid at room temperature until completely dissolved and titrated with 0.5 M sodium hydroxide at 25 °C. Sodium hydroxide solution was added in portions of 0.2 mL in interval of 20 s added in portions of 0.2 mL in interval of 20 s. The values of conductance (mS.cm<sup>-1</sup>) with the corresponding titrant volumes were plotted in a graphic to find the linear variation before and after the equivalence point. The degree of deacetylation (DD) was calculated using the following equation (1):

$$DD = \frac{[base](V_2 - V_1)161}{m}$$

where [base] is the concentration of the sodium hydroxide solution; V<sub>1</sub> and V<sub>2</sub> are the volumes of sodium hydroxide (mL) used in the titration in two inflection points; 161 is the molar mass of the glucosamine monomer (C<sub>6</sub>H<sub>11</sub>O<sub>4</sub>N) and *m* is the mass of chitosan (mg).

### Synthesis of CMC

Synthesis of CMC was prepared from chitosan as described previously (Chen and Park, 2003; Miao *et al.*, 2006; Bidgoli *et al.*, 2010). Briefly, chitosan (2 g) suspended in 50 % (w/v) sodium hydroxide (20 mL) was left swelling for 1 h at room temperature and kept at -20 °C for alkalization for 12 h, then thawed at room temperature. The alkali chitosan was suspended into 2-propanol (50 mL) and the mixture was stirred on magnetic stirrer for 30 min and then in water bath shaker at 50 °C. Chloroacetic acid (10 g) dissolved in isopropanol (30 mL) was added by drops over a period of 30 min. The reaction mixture was stirred for 12 h in a water bath at 50 °C. Then the liquid fraction was decanted and methanol (100 mL) was added to the resulting slurry. The suspension was neutralized using glacial acetic acid.

Then the mixture was filtered and washed several times with methanol. The resulting CMC was purified by dissolving in deionized water and filtered to remove undissolved residues. The resultant solution was precipitated in addition of methanol. Finally the pure product was separated by filtration, rinsed with methanol, vacuum freeze dried and stored in a desiccator until further use.

### Characterization of CMC

#### Degree of substitution

The degree of substitution of CMC was determined by potentiometric titration (Hua-Cai and Deng, 2005). CMC was dissolved in distilled water and the solution was adjusted to pH < 2 by addition of hydrochloric acid. Then, the CMC solution was titrated with 0.1 M aqueous sodium hydroxide and the pH value of the solution was simultaneously recorded. The amount of aqueous sodium hydroxide was determined by the second order differential method. The degree of substitution (DS) was calculated as follows:

$$DS = \frac{161 \cdot A}{m_{CMC} - 58 \cdot A}$$

$$A = V_{\text{sodium hydroxide}} \times C_{\text{sodium hydroxide}}$$

where  $V_{\text{sodium hydroxide}}$  and  $c_{\text{sodium hydroxide}}$  are the volume and molarity of aqueous sodium hydroxide, respectively;  $m_{CMC}$  is the mass of CMC (g), and 161 and 58 are the molecular weight of glucosamine (chitosan skeleton unit) and a carboxymethyl group, respectively (Mourya *et al.*, 2010).

#### FTIR-spectroscopy

The FTIR spectra of chitosan and the sodium salt of CMC were recorded on Nicolet Avatar 330 FT-IR, Termo Science, (USA) spectrophotometer in KBr pellets. The scanning range was 400 – 4000  $\text{cm}^{-1}$  with 132 scans at 4  $\text{cm}^{-1}$  resolution.

#### NMR spectroscopy

The  $^{13}\text{C}$  NMR spectra of chitosan and CMC were recorded on a Bruker AVIII 500M spectrometer using polymer samples in form of sodium salts dissolved in  $\text{D}_2\text{O}$  (for CMC) and in  $\text{CD}_3\text{COOD}$  (for chitosan) at a concentration of 40 mg/mL. All chemical shifts were given relative to a tetramethylsilane (TMS) as internal standard.

#### Thermal analysis (TGA/DTA)

The thermophysical properties of chitosan and CMC were investigated by differential thermal analysis-thermogravimetric analysis (DTA-TG) using LABSY TM Sevo (Setaram, France). The DTA-TG curves were obtained during heating of the samples with a heating rate of 5  $^{\circ}\text{C}/\text{min}$  from 10  $^{\circ}\text{C}$  to 400  $^{\circ}\text{C}$  under nitrogen atmosphere (Murdzheva *et al.*, 2016).

#### Preparation of the oil/water pharmaceutical and cosmetic emulsions

The *phase I* contained the following ingredients with (INCI) names: 1. Emulgade<sup>®</sup> SE (Glyceryl Stearate (and

Ceteareth-20 (and) Ceteareth-12 (and) Cetearyl Alcohol (and) Cetyl Palmitate – 6%; 2. Lanette<sup>®</sup> O (Cetearyl Alcohol) – 2%; 3. Cera Alba – 1%; 4. Parafinumliquidum – 6%; 5. Caprylic/Capric Triglyceride – 6.5%; 6. Isopropyl Myristate – 6%; 7. Nipagin<sup>®</sup> (Methyl paraben) – 0.2 %; 8. Nipasol<sup>®</sup> (Propyl paraben) – 0.1 %.

The *phase II* contained: 1. Glycerol – 4.0 %; 2. Aqua – to 100 %.

The *phase III* contained: 1. Carbopol<sup>®</sup> Ultrez 21 (Carbomer) – 0.30% (control – emulsion 1); CMC – 0.5 % (emulsion 2) and CMC – 0.3 % (emulsion 3).

The *phase IV* contained: Triethanolamine – 0.3 % (emulsion 1)

The *phase V* contained: 1. Bronopo<sup>®</sup> (2-Bromo-2-Nitropropane-1,3-Diol) – 0.05%; 2. Rosa damascena Absolute – 0.3% (perfume and active ingredient).

In all variants the *phases I* was heated at 80 – 85  $^{\circ}\text{C}$ . The *phase III* was added into the *phase II* under stirring. *Phase II* was heated at 80 – 85  $^{\circ}\text{C}$  and then added to *phase I* and the resulting mixture was homogenized with laboratory homogenizing device Polytron<sup>®</sup>PT45-80 (Kinematika, Switzerland) with technical characteristics – 1600 W, max 250  $\text{s}^{-1}$  for 2 min. The emulsions obtained were cooled. The *phase IV* was added into the hot emulsion (60  $^{\circ}\text{C}$  for emulsion 1) and homogenized. The prepared emulsions were allowed to cool with stirring in such a way that it remains in continual motion as avoiding the incorporation of air. The *phase V* was added at 40  $^{\circ}\text{C}$ .

#### Determination of pH

The acidity of the emulsions has been determined by pH meter Hanna HI 98127 with replaceable electrode.

#### Determination of emulsion stability

The long-term emulsion stability was determined by centrifuge test according to the procedure of Tcholakova *et al.* (2004).

#### Microscopic Test

The microstructure of the emulsions was investigated by microscope Olympus BX41 (USA), equipped with USB camera connected to a personal computer. The drop sizes distribution was observed at magnification  $\times 1000$ .

#### Determination of emulsion turbidity

The investigations were performed by CamspecM107 (UK) Double Beam Scanning UV/VIS spectrophotometer. Series of standard emulsion solutions were placed into a disposable spectrophotometer cuvette (1 mL) and the change of the emulsion turbidity were measured in a range of 375 – 405 nm (Gandova and Balev, 2016). Thermodynamic parameters (Gibbs free energy, enthalpy and entropy) of the emulsions were calculated by the equation (3):

$$\frac{d \ln K}{d(1/T)} = \frac{-\Delta H}{R}$$

For Gibbs free energy and entropy determination were used the classical thermodynamic equations (4) and (5):

$$\Delta G = -RT \ln K$$

$$\Delta S = \frac{(\Delta H - \Delta G)}{T}$$

where  $\Delta H$  – enthalpy ( $\text{kJ}\cdot\text{mol}^{-1}$ ),  $\Delta G$  – Gibbs free energy ( $\text{kJ}\cdot\text{mol}^{-1}$ ),  $\Delta S$  – entropy ( $\text{kJ}\cdot\text{K}^{-1}\cdot\text{mol}^{-1}$ ),  $R$  – universal gas constant ( $R = 8.314\text{J}\cdot\text{K}^{-1}\cdot\text{mol}^{-1}$ ),  $T$  – absolute temperature (K),  $K$  – equilibrium constant.

### Rheological behavior

The rheological behavior of the prepared emulsions was studied on a rotary viscometer "Brookfield" RV DV-II + Pro, equipped with an adapter for small samples, comprising a metal cylinder measuring with a water jacket SC4-13R and a cylindrical spindle with conical head SC4-27 (a length of the tube 33.02 mm and diameter 11.76 mm and total length of the working part 39.29 mm). The measuring cylinder had an internal diameter of 19.05 mm and a length of 64.77 mm. The upper conical part of the spindle should cover the test product. Therefore, during each experiment, the cylinder was filled with emulsion volume of 10.4 mL. Before the start of measurement, an insulating cap was placed on the neck of cylinder, and then began the preliminary experiments in order to specify the range of shear rates in which the measurements were possible to be done. The water jacket of the adapter for small samples was connected by flexible connections with ultra-thermostat "Zemal Horizont", equipped with a contact thermometer with a range from 0 to 100 °C  $\pm$  0.1 and second control thermometer with the same scope. The measuring cylinder was filled with emulsion and then heated at four different temperatures (20, 25, 30 and 35 °C, respectively) for a period of 5 min. The selected temperatures were concerned with the storage and stability conditions of emulsions. After reaching the required temperature, an insulating cap was placed on the neck of the cylinder, and then the experiments can be started. An experiment was designed, during which the structural and mechanical properties of each emulsion were measured at 28 shear rates ( $D = 0.1 \div 1.02 \text{ s}^{-1}$ ) determined during the preliminary experiments. Each experiment continued 42 min - the spindle rotated at every shear rates for the period of 90s at the end of which the viscometer registered a reading. The resulting data were used for constructing graphical dependencies between the shear stress and the shear rate which were used to define the rheological properties of the emulsion. The average values of the results from

the experiments were approximated by the rheological model of Herschel-Bulkley equation (6) which has the highest R-squared coefficients. The same file presented also graphical dependencies between shear rate and apparent viscosity and between shear rate and shear stress for the individual emulsions at all tested temperatures.

$$\tau = \tau_0 + k \cdot D^n \quad (6)$$

where  $\tau$  – shear stress, Pa;  $\tau_0$  – yield stress, Pa;  $k$  – consistency index,  $\text{Pa}\cdot\text{s}^n$ ;  $D$  – shear rate,  $\text{s}^{-1}$ ;  $n$  – flow index.

## RESULTS AND DISCUSSION

### Characterization of CMC

General reaction scheme for synthesis of CMC with monochloroacetic acid in 50 % sodium hydroxide was shown (Fig. 2). The resulting yield of CMC was 2.4 g or 83% on the base of used chitosan. The synthesized CMC with DS 50 % demonstrated good water solubility that is an important characteristic for this chitosan derivate. Our findings were in agreement of Chen *et al.* (2005), who recognized that the DS value in the range of 0.40 to 0.45 became CMC soluble in water. Water solubility of CMC plays significant role in application of CMC, especially for drug delivery systems and strongly depends on concentration of sodium hydroxide used in reaction conditions (Mourya *et al.*, 2010). In our case modification of chitosan with 50 % sodium hydroxide at lower temperature gave CMC with DS 50 %. A 50 % sodium hydroxide solution seemed to provide the optimum alkali concentration in the carboxymethylation process (Mourya *et al.*, 2010).

Our results proved that CMCs prepared at temperatures of 50 °C were soluble in water (Ali *et al.*, 2013; Bidgoli *et al.*, 2010; Chen and Park, 2003). Compared with chitosan, the solubility of CMC in aqueous solution could be explained with the introduction of carboxymethyl group. DS is important parameter, which could influence its performance in many of its applications. Other physicochemical parameters of CMC were summarized in Table 1.

**Table 1:** Comparative characteristics of chitosan and carboxymethyl chitosan

Characteristic	Chitosan	CMC
Appearance	fine powder	fine powder
Colour	pure white	pure white
Odour	no	no
Degree of deacetylation, %	79	-
Degree of substitution, %	-	50
Solubility	in acidic medium	in water

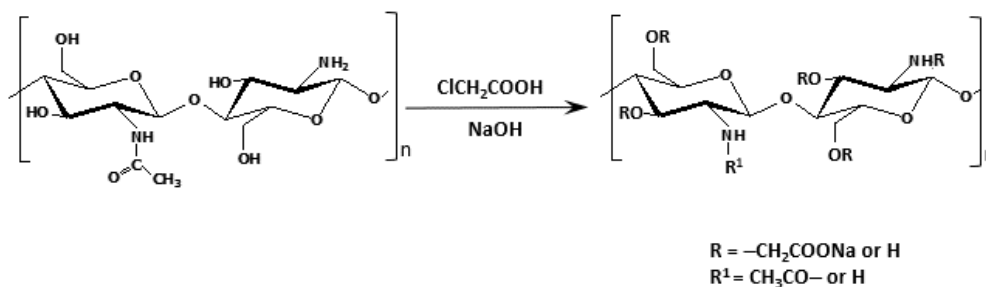


**Fig. 2:** General reaction scheme for synthesis of CMC.

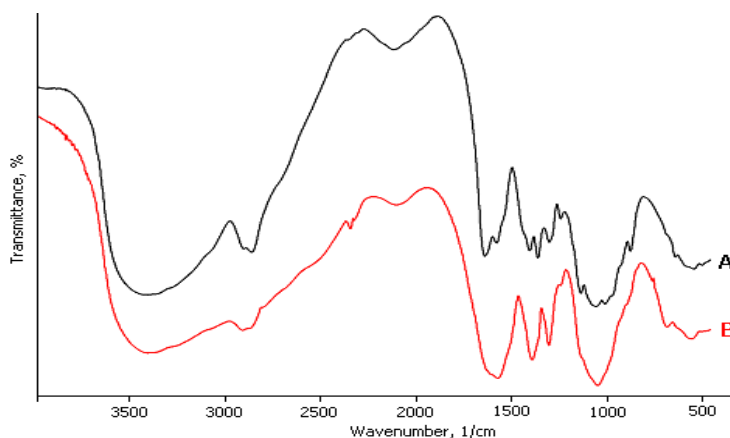


Fig. 3: FTIR – spectra of chitosan (A) and CMC (B).

### FTIR-spectroscopy

The carboxymethylation provoked structural changes that were clearly identified by comparing the FTIR spectra of chitosan and CMC (Fig. 3).

As it was shown (Fig.3), both spectra showed a broad absorption band between  $3500\text{ cm}^{-1}$  and  $3100\text{ cm}^{-1}$ , due to O–H stretching vibrations, N–H extension vibration and the intermolecular H-bonds of the polysaccharide moieties, respectively. The occurrence of a broader band at  $3419\text{ cm}^{-1}$  revealed a more hydrophilic character of CMC as compared to the initial chitosan (Fig.2B). Therefore, carboxylation occurred on some of both the amino and the primary hydroxyl moieties of the glucosamine units of the chitosan structure (Miao *et al.*, 2006) and we can conclude that the structure is N,O-CMC. The band at  $2926\text{ cm}^{-1}$  could be assigned to  $\nu(\text{C-H})$  from  $\text{CH}_2$  groups. The increase in width of the bands at  $2960\text{ cm}^{-1}$  and  $2930\text{ cm}^{-1}$  was assigned to C–H stretching and asymmetric deformations in  $\text{CH}_2$ . The asymmetric stretching vibration of the carboxylate group appears at  $1620\text{--}1598\text{ cm}^{-1}$ .

The introduction of carboxymethyl groups was confirmed by the occurrence of an intense band at  $1589\text{ cm}^{-1}$  and a moderate band at  $1409\text{ cm}^{-1}$ . These bands were attributed to symmetric and asymmetric deformation of  $\text{COO}^-$ , respectively (Hua-Cai and Deng-Ke, 2005). A band at  $1589\text{ cm}^{-1}$  was attributed to the angular deformation of the N–H bonds of the amino group, which overlaps with  $\nu_{as}(\text{COO}^-)$  and  $\nu_s(\text{COO}^-)$ . The new bands at  $1413\text{ cm}^{-1}$  were observed in CMC FTIR spectra. Moreover, the bands at  $1597\text{--}1650\text{ cm}^{-1}$  and  $1414\text{--}1401\text{ cm}^{-1}$  corresponding to the carboxy group (which overlaps with N–H bend) and  $-\text{CH}_2\text{COOH}$  group respectively were intense in the spectrum of CMC indicating carboxymethylation on both the amino and hydroxyl groups of chitosan. The bands in the range  $1417\text{--}1377\text{ cm}^{-1}$  were assigned with coupling of C–N stretching and N–H angular deformation (Mourya *et al.*, 2010). Additionally, the formation of CMC was also confirmed by the intensification of the band at  $1067$  and  $1323\text{ cm}^{-1}$  corresponding to  $\nu(\text{C-O-C})$  and  $\nu_s(\text{C-OH})$ . The stretching vibrations in the range of  $1154\text{--}1029\text{ cm}^{-1}$  were assigned with glycosidic bonds, C–O–C and C–O

symmetric stretching vibrations from the pyranose ring. The C–O stretching band at  $1028\text{ cm}^{-1}$  corresponding to the primary hydroxyl group disappears, verifying a high carboxymethylation of OH-6 (Zhang *et al.* 2000; Zhao *et al.*, 2001; Meiling *et al.*, 2011). In chitosan and CMC the bands at  $989$  and  $943\text{ cm}^{-1}$  were attributed to the C–O stretching vibration of the pyranosyl ring and the C–O stretching with contributions from C–C–H and C–O–H deformation. In chitosan spectra a band at  $892\text{ cm}^{-1}$  was due to C-anomeric group stretching, C–1–H deformations and pyranosyl ring stretching.

### $^{13}\text{C}$ NMR spectra

Structure of chitosan and CMC were characterized by  $^{13}\text{C}$  NMR spectroscopy. Chitosan  $^{13}\text{C}$  NMR (151 MHz,  $\text{CD}_3\text{COOD}$ ) chemical shifts were:  $\delta$  175.20, 99.42 (C-1), 78.07 (C-4), 74.71 (C-5), 72.50 (C-3), 69.69, 67.28, 66.59 (C-6), 54.54 (C-2), 13.89 ppm

$^{13}\text{C}$  NMR spectra of chitosan consisted of eight well-defined resonances. Six signals in the range from 50 to 105 ppm were due to carbon atoms from the glucosamine pyranose ring. The single signal at 175.20 ppm was assigned to the carbonyl carbons of carboxyl groups. The shifts at 13.89 ppm were due to  $\text{CH}_3$  from acetyl residues. The reported chemical shifts in our study were consistent to the reported ones by Cárdenas *et al.* (2006).

CMC Chitosan  $^{13}\text{C}$  NMR (126 MHz,  $\text{D}_2\text{O}$ ) 178.04, 177.78, 175.94, 171.35, 101.51 (C-1), 78.40 (C-4), 77.98 (C-5), 73.89 (C-3), 70.29, 69.48, 61.19 (C-6), 60.02 (C-2), 57.41, 30.22, 16.76 ppm.

The methylene groups ( $-\text{CH}_2-$ ) from carboxymethyl residues  $\text{OCH}_2\text{COOH}$  gave the signals at 57.41 ppm and also in the range between 67 and 74 ppm. The signal at 101.51 ppm was typical for  $\beta$  anomers in the polysaccharide chain. Moreover, the signal observed at 178.04 ppm was assigned to the carbonyl carbons of carboxymethyl groups. Chemical shifts at 177.78 ppm corresponded to the carbonyl carbon of  $-\text{COCH}_3$  of the parent chitosan. The shifts at 175.94 ppm can be assigned with C=O substituted on  $-\text{OH}$ . The presence of shifts at 170 ppm and a weak

signal at 57.41 ppm proved that  $-\text{CH}_2\text{COOH}$  was bonded to  $-\text{NH}_2$  groups of chitosan. The presence of chemical shifts at 70.29 and 69.48 ppm proved that substitution with  $\text{CH}_2\text{COO}$  residues was occurred on O-6 and O-3 positions in pyranose units. The signal around 16.76 ppm, corresponding to  $-\text{CH}_3$  groups can be associated with presence of residual methanol used as a solvent for sample purification.

No significant differences between  $^{13}\text{C}$  NMR spectra of chitosan and CMC presented in our study and the previously reported ones by some authors (Mourya *et al.*, 2010; de Abreu and Campana-Filho, 2005).

### Thermal analysis of chitosan and CMC polymers

The TGA and DTA curves of initial chitosan and carboxymethyl chitosan were shown (Fig.4 and Fig. 5). Chitosan (Fig.4) exhibited one-stage degradation behavior. The mass loss of 7.4 % for chitosan was observed in the temperature range of 38 - 132 °C. That was associated with the endothermic peak due to loss of capillary bonded water. The thermogravimetric curve from TG analysis indicated the presence of an inflection point at 90 °C which showed a highly elastic state and could be considered as

glass transition temperature. No degradation processes in chitosan thermogram were observed by 240 °C and that temperature could be defined as the limit of thermal stability of chitosan.

In CMC DTA thermogram (Fig. 5), the endothermic transition due to the evaporation of the capillary bounded water was observed at the same temperature of 36 °C and ended significantly faster at 102 °C with a peak at 76 °C. The inflection point was at 75 °C. Although the evaporation temperature range for was narrow, the released water was about 10% of tability of CMC the mass of the sample. The thermal was until 220 °C, after which exothermic transition was recorded beginning at 221 °C and end at 259 °C with a maximum at 236 °C. The onset of these pyrolytic degradation processes resulted from the decarboxylation of the acetate residues, whereby the mass lost was about 29%. The similar observation was reported for other modified carbohydrate polymers (Murdzheva *et al.*, 2016). After TGA/DTA analysis can be concluded that CMC is suitable to be used in heating and sterilization processes up to 220 °C without changing the quality composition. All these observations revealed the higher thermal stability of synthesized CMC for potential application in food processing and pharmaceutical preparations.

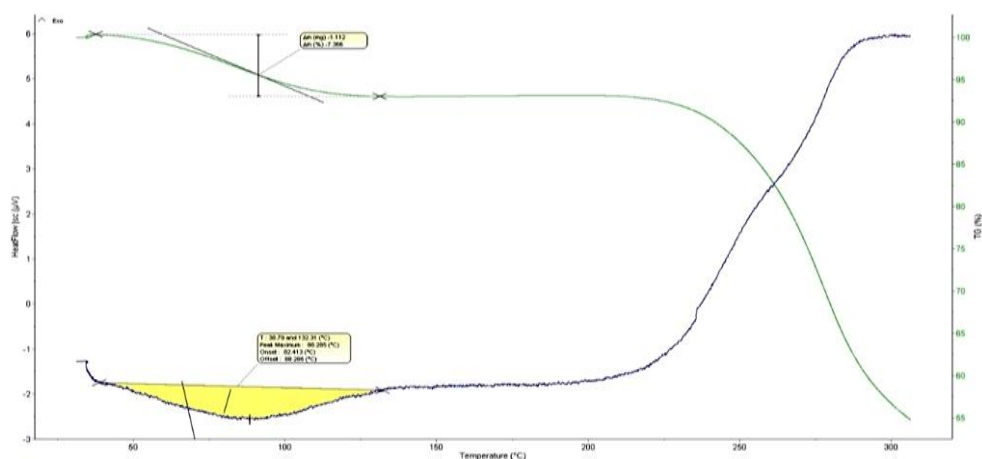


Fig. 4: TGA/DTA analyses of chitosan.

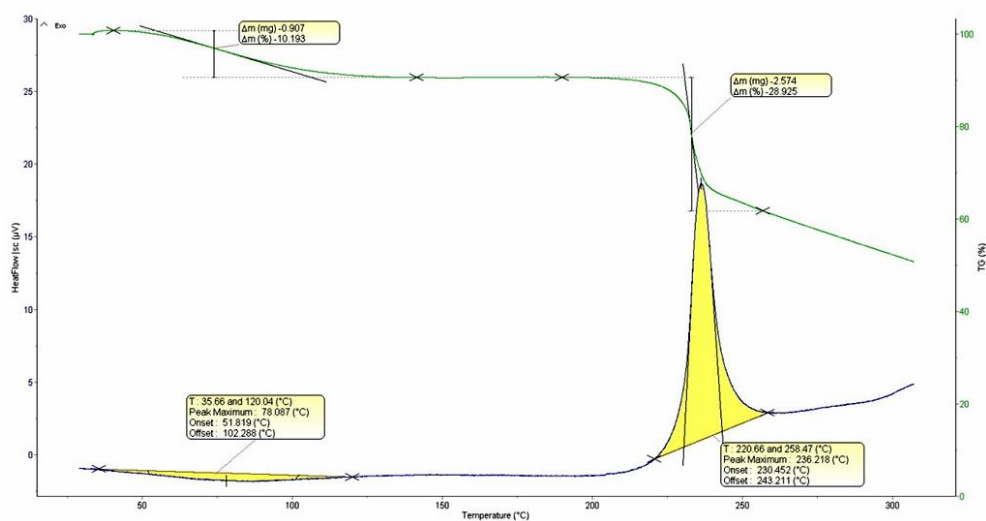


Fig. 5: TG/DTA analyses of CMC.

## Emulsions

The synthesized CMC was incorporated in different concentration in oil/water emulsions. The resulting emulsions represented yellow-colored viscous mixtures with intense and typical rose odour and pH values measured in a range of 6.45 to 7.33. The results obtained by centrifugation showed that emulsions are stable in the range of 20 – 26 months.

The microscopy images of emulsions 1, 2 and 3 after three days storage are shown (Fig. 6). An important parameter for emulsion stability is droplets size determination and their distribution in the continuous phase (McClements, 2005). The average radius of emulsion droplets has been calculated. The image of emulsion 1 showed a homogeneous structure with approximately equal droplets size ( $r=14.23 \mu\text{m}$ ). The small particles size was associated with greater dispersion system stability. Microscopic images of emulsions 2 and 3 showed larger emulsion droplets ( $38.73\mu\text{m}$  and  $46.97 \mu\text{m}$ ) compared to emulsion 1. But they were similarly stable and that was confirmed by the results obtained for thermodynamic parameters shown in Table 2. Thermodynamic parameters of emulsions have been calculated and their values were presented in Table 2.

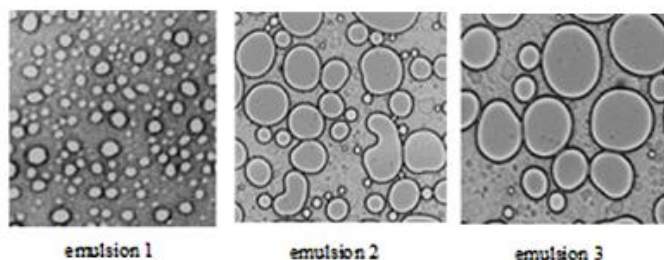


Fig. 6: Microscopy images of the structure of model oil/water emulsions.

Table 2: Thermodynamic parameters obtained in emulsions at 298.2 K.

Emulsion	$\Delta G$ [kJ mol <sup>-1</sup> ]	$\Delta H$ [kJ mol <sup>-1</sup> ]	$\Delta S$ [kJ mol <sup>-1</sup> K <sup>-1</sup> ]	K
1	-11.3±0.4	-22.2±0.6	-0.0367±0.0012	96.8±3.3
2	-10.7±0.4	-22.0±0.6	-0.0379±0.0012	75.2±8.7
3	-10.6±0.5	-21.9±0.7	-0.0303±0.0010	74.0±7.4

The thermodynamic parameters (Gibbs free energy, enthalpy and entropy) and the equilibrium constant of the process were calculated by spectrophotometric method. They are indicators for system stability. The highest value of the constant was observed for emulsion 1, therefore it was evaluated as the most stable compared to another two. The value of equilibrium constants for emulsion 2 and 3 were approximately similar and they were similarly stable in thermodynamic terms.

The relationship between K and the energy of Gibbs was proportional. It was observed that  $\Delta G < 0$  for the analyzed emulsions (Table 2).  $\Delta G$  was in the range of -10.6 and -11.3 kJ.mol<sup>-1</sup>. The same results in terms of stability were established by microscopic analysis (Fig. 6).

Calculated enthalpies of the three emulsions had relatively high negative values. It was connected with strong endothermic processes, which shifts the equilibrium towards the formation of the products (in this case - towards the stable emulsion formation).

Entropy in each emulsion system had low negative value close to zero and did not affect the direction of the process. This means that the system will long be regarded as an emulsion.

## Rheological behavior

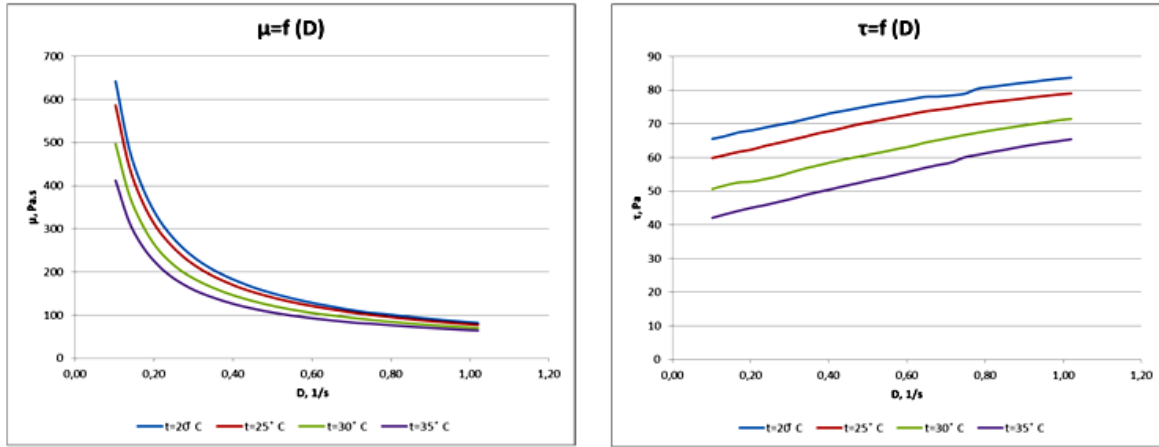
All tested emulsions (Table 3) behaved like Herschel-Bulkley visco-plastic fluids, but they were also closed to the Bingham plastics (the flow index (n) had values above 0.5 – from 0.57 to 0.87, with two exceptions). In the Bingham model flow index (n) is always equal to 1.

The apparent viscosity ( $\mu$ ) decreased with increasing number of the emulsions. For emulsion 1 (control) it was in the range of 642 to 64.2 Pa.s; for emulsion 2 with 0.5% CMC – from 442.5 to 42.8 Pa.s; for emulsion 3 with 0.3 % CMC – from 224.2 to 31.1 Pa.s (Fig. 7).

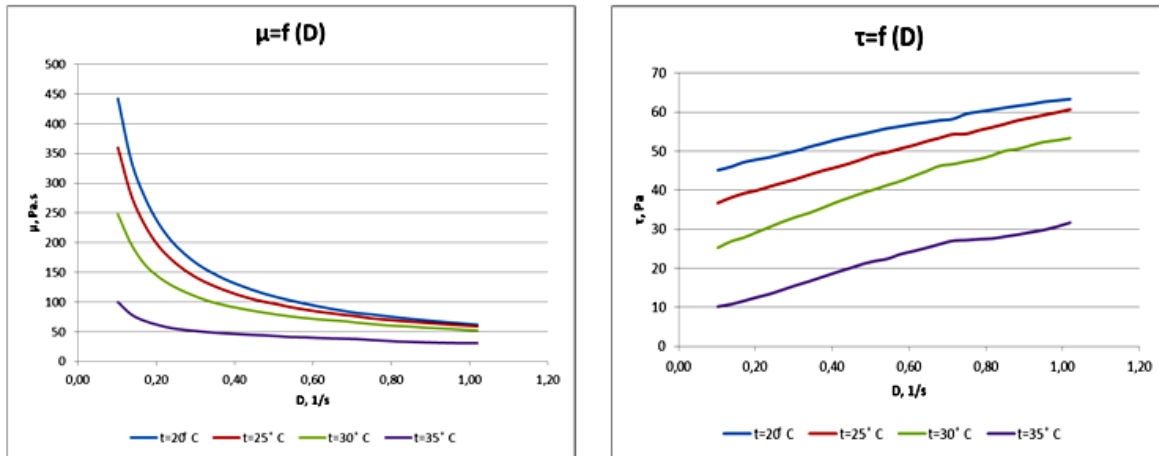
By increasing the temperature of each emulsions, viscosity and shear stress decreased with different gradient – the highest for emulsion 3 – 55.4 % (for emulsion 1 – 35.8%, for emulsion 2 – 49.0 %). The same case happened with a large shear rate – emulsion 3 – 42.9%, emulsion 2 – 31.0% and emulsion 1 – 21.8%. The use of CMC as a thickening agent implies good knowledge of their rheological characteristics. The emulsions containing 0.5 % and 0.3 % CMC could be applied in pharmaceutical and cosmetic formulations.

Table 3: Rheological characteristics of emulsion systems.

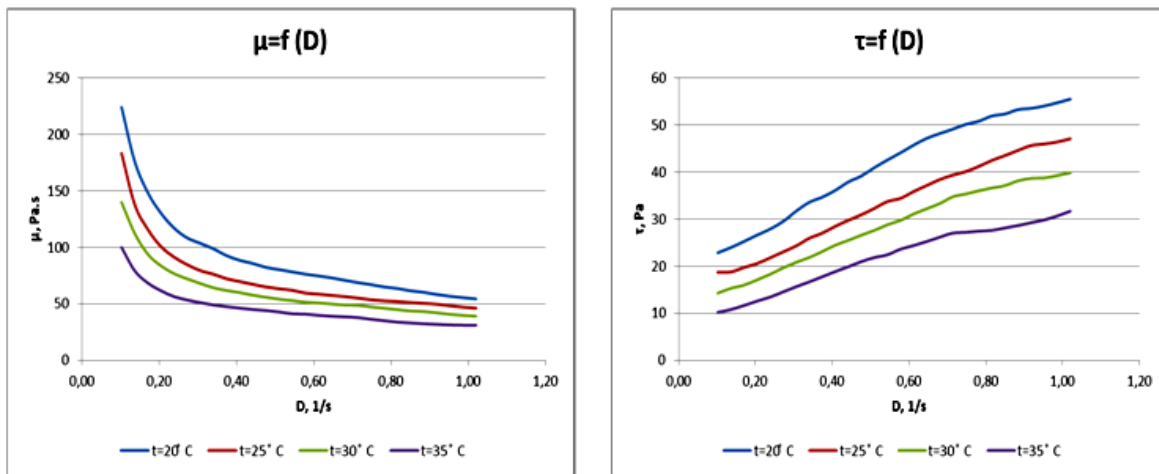
Emulsion	D = 0.1 – 1.02 s <sup>-1</sup>											
	t=20°C			t=25°C			t=30°C			t=35°C		
	$\tau_0$ , Pa	k, Pa.s <sup>n</sup>	n	$\tau_0$ , Pa	k, Pa.s <sup>n</sup>	n	$\tau_0$ , Pa	k, Pa.s <sup>n</sup>	n	$\tau_0$ , Pa	k, Pa.s <sup>n</sup>	n
1	60.0	23.7	0.66	51.7	27.6	0.57	46.1	25.6	0.80	38.2	27.4	0.87
2	39.5	23.9	0.65	31.6	28.8	0.77	16.6	36.9	0.66	10.7	33.6	0.47
3	10.7	33.6	0.47	7.78	48.6	0.57	5.85	34.8	0.68	0.8	30.5	0.57



Emulsion 1 (control)



Emulsion 2



Emulsion 3

Fig. 7: Viscosity ( $\mu$ ) and shear stress ( $\tau$ ) of emulsions with CMC as a function of shear rate ( $D$ ).



## CONCLUSION

Carboxymethyl chitosan with 50 % degree of substitution was successfully synthesized. The resulting product was characterized by FTIR and NMR spectroscopy and TGA. Carboxymethylchitosan is water soluble polymer with high viscosity in resulting solutions and could be successfully used in pharmaceuticals and cosmetics as emulsion stabilizer and thickening agent. The thermodynamic parameters of emulsions (Gibbs free energies, enthalpies and entropies) and rheological properties indicate that the carboxymethylchitosan synthesized by us can successfully replace the stabilizer Carbomer that has traditionally been used in pharmaceutical and cosmetic oil/water emulsions. Some important rheological parameters like creep recovery, spreadability and etc. will be an object for future investigations.

**Financial support and sponsorship:** Nil.

**Conflict of Interests:** There are no conflicts of interest.

## REFERENCES

- Ali Z, Laghari A, Ansari A, Khuhawar M. Synthesis and characterization of carboxymethyl chitosan and its effect on turbidity removal of river water. *J. Appl. Chem.* 2013; 5(3):72-79.
- Bigdoli H, Zamani A, Taherzadeh M. Effect of carboxymethylation conditions on the water-binding capacity of chitosan-based superabsorbents. *Carbohydr. Res.* 2010; 345 (18):2683-2689.
- Cárdenas G, Cabrera G, Taboada E, Rinaudo M. Synthesis and characterization of chitosan alkyl phosphate. *J. Chil. Chem. Soc.* 2006; 51(1):815-820.
- Chen L, Du Y, Tian Z, Sun L. Effect of the degree of deacetylation and the substitution of carboxymethyl chitosan on its aggregation behavior. *J. Polym. Sci. Polym. Phys.* 2005; 43:296-305.
- Chen X, Park H. Chemical characteristics of O-carboxymethyl chitosans related to the preparation conditions. *Carbohydr. Polym.* 2003; 53(4):355-359.
- Cochran S, Brockman T. A cosmetic ingredient innovation for the stabilization and delivery of volatile fluoroether with cosmetic applications. *J. Cosmet. Sci.* 2007; 58:413-419.
- Cravotto G, Tagliapietra S, Robaldo B, Trotta M. Chemical modification of chitosan under high-intensity ultrasound. *Ultrason. Sonochem.* 2005;12: 95-98.
- de Abreu F, Campana-Filho S. Preparation and characterization of carboxymethylchitosan. *Polímeros: Ciência e Tecnologia* 2005; 15(2):79-83.
- Ewing G. 1969. Instrumental methods of chemical analysis. New York, McGraw-Hill.
- Gandova V, Balev D. Properties of emulsions based in soybean oil stabilized by different proteins. *Int. J. Inn. Sci. Eng. Technol.* 2016; 3(5):293-297.
- Holme K, Perlin A. Chitosan N-sulfate. A water-soluble polyelectrolyte. *Carbohydr Res.* 1997; 302(1-2):7-12.
- Hua-Cai G, Deng-Ke L. Preparation of carboxymethyl chitosan in aqueous solution under microwave irradiation. *Carbohydr. Res.* 2005; 340:1351-1356.
- Jia Z, Shen D, Xu W. Synthesis and antibacterial activities of quaternary ammonium salt of chitosan. *Carbohydr. Res.* 2001; 333(1):1-6.
- Jimtaisong A, Seawan N. Utilization of carboxymethyl chitosan in cosmetics. *Int. J. Cosmet. Sci.* 2014; 36:12-21.
- Jung B, Kim C, Chio K, Lee Y, Kim J. Preparation of amphiphilic chitosan and their antimicrobial activities. *J. Appl. Polym. Sci.* 1999; 72 (13):1713-1719.
- Kasaai M, Arul J, Charlet G. Fragmentation of chitosan by acids. *The Scientific World Journal* 2013; 1-11.
- Kim S, Shin S, Lee Y, Kim S. Swelling characterizations of chitosan and polyacrylonitrile semi-interpenetrating polymer network hydrogels. *J. Appl. Polym. Sci.* 2003; 87:2011-2015.

Kurita K. Controlled functionalization of the polysaccharide chitin, *Progress in Polymer Science* 2001; 26:1921-1971.

Lee S, Liu K, Liu Y, Chang Y, Lin C, Chen Y. Chitosonic® acid as a novel cosmetic ingredient: Evaluation of its antimicrobial, antioxidant and hydration activities. *Materials* 2013; 6:1391-1402.

Lei CX, Hu SQ, Shen GL, Yu RQ. Immobilization of horseradish peroxidase to a nano-Au monolayer modified chitosan-entrapped carbon paste electrode for the detection of hydrogen peroxide. *Talanta* 2003; 59:981-993.

McClements D. 2005. Food emulsions: principles, practice and techniques, 2nd edition, Boca Raton: CRC Press

Meiling Z, Baoqin H, Yan Y, Wanshun L. Synthesis, characterization and biological safety of O-carboxymethyl chitosan used to treat Sarcoma 180 tumor. *Carbohydr. Polym.* 2011; 86:231-238.

Miao J, Chen G, Gao C, Lin C, Wang D, Sun M. Preparation and characterization of N, O-carboxymethyl chitosan (NOCC)/polysulfone (PS) composite nanofiltration membranes. *J. Membrane Sci.* 2006; 280:478-484.

Mourya V, Inamdar N. Trimethyl chitosan and its applications in drug delivery. *J. Mater. Sci. Mater. Med.* 2009; 20:1057-1079.

Mourya V, Inamdar N., Tiwari A. Carboxymethyl chitosan and its applications. *Advanced Materials Letters* 2010; 1(1):11-33.

Mourya VK, Inamdar NN. Chitosan-modifications and applications: opportunities galore. *React. Funct. Polym.* 2008; 68(6):1013-1051.

Murdzheva D, Petkova N, Todorova M, Vasileva I, Ivanov I, Denev P. Microwave-assisted synthesis of methyl esters of alginic acids as potential drug carrier. *Int. J. Pharmac. Clinical Res.* 2016; 8(10):1361-1368.

Muzzarelli R. Carboxymethylated chitins and chitosans. *Carbohydr. Polym.* 1988; 8:1-21.

Ouchi T, Nishizawa H, Ohya Y. Aggregation phenomenon of PEG-grafted chitosan in aqueous solution. *Polymer* 1998; 39:5171-5175.

Park IK, Kim TH, Kweon HY, Park YH, Kim WJ, Akaike T, Cho CS. Visualization of transfection of galactosylated chitosan-graft-poly(ethylene glycol) /DNA complexes into hepatocytes by confocal laser scanning microscopy. *Int. J. Pharm.* 2003; 257:103-110.

Patravale V, Mandawgade S. Novel cosmetic delivery systems: An application update. *Int. J. Cosmet. Sci.* 2008; 30:19-33.

Sashiwa H, Kawasaki N, Nakayama A, Muraki E, Yajima H, Yamamori N, Ichinose Y, Sunamoto J, Aiba S. Chemical modification of chitosan. Synthesis of novel chitosan derivatives by substitution of hydrophilic amine using N-carboxyethylchitosan ethyl ester as an intermediate. *Carbohydr. Res.* 2003; 338(6):557-561.

Shanmuganathan S, Nigma Chandra S, Anbarasan B, Harika B. Preparation and *in-vitro* evaluation of Fe<sub>3</sub>O<sub>4</sub> encapsulated by chitosan loaded capcitabine nanoparticles for the treatment of breast cancer. *J. Drug Delivery Techn.* 2016; 6(3):52-57.

Sharma D., Dhanjal D. S., Mittal B. Development of Edible Biofilm Containing Cinnamon to Control Food-Borne Pathogen. *Journal of Applied Pharmaceutical Science* 2017; 7 (01): 160-164.

Tcholakova S., N. Denkov, I. Ivanov, R. Marinov. Evaluation of Short-Term and Long-Term Stability of Emulsions by centrifugation and NMR. *Bulg. J. Phys.* 2004; 31: 96-100.

Yalpani M, Marchessau R, Morin F, Monasterios C. Synthesis of poly(3-hydroxyalkanoate) (PHA) conjugates: PHA-carbohydrate and PHA-synthetic polymer conjugates. *J. Macromolecules* 1991; 24:6046-6049.

Yang C, Chen Y, Lai J, Hong W, Lin C. Determination of the thermodegradation of deoxyarbutin in aqueous solution by high performance liquid chromatography. *Int. J. Mol. Sci.* 2011; 11:3977-3987.

Zhang L, Guo J, Zhou J, Yang G, Du Y. Blend membranes from carboxymethylated chitosan/alginate in aqueous solution. *J. Appl. Polym. Sci.* 2000; 77(3):610-616.

Zhao X, Kato K, Fukumoto Y, Nakamae K. Synthesis of bioadhesive hydrogels from chitin derivatives. *Int. J. Adhesion and Adhesives.* 2001; 21(3): 227-232.

### How to cite this article:

Tzaneva D, Simitchiev A, Petkova N, Nenov V, Stoyanova A, Denev P. Synthesis of Carboxymethyl Chitosan and its Rheological Behaviour in Pharmaceutical and Cosmetic Emulsions. *J App Pharm Sci*, 2017; 7 (10): 070-078.